Supporting Information

An engineered peptide-polymer conjugate mimics statherin to block dental calculus formation while preserving oral microbiota

Qiangwei Xin,[a] Li Li,[a] Peng Yu,[a] Yao Zhao,[a] Zhengxin Ma,[a] Hongbo Zhang,[a] Shiran Sun,[a] Jun Luo,[a] Liwei Zheng,[b] Chunmei Ding,*[a] Yang Liu,*[a] Mingming Ding[a] and Jianshu Li*[a]

[a] College of Polymer Science and Engineering, National Key Laboratory of Advanced Polymer Materials, Sichuan University, Chengdu 610065, China
[b] State Key Laboratory of Oral Diseases, West China Hospital of Stomatology, Sichuan University, Chengdu 610041, China
[c] Med-X Center for Materials, Sichuan University, 610041, China
* Author for correspondence:
Chunmei Ding, Ph.D
E-mail address: dingcm@scu.edu.cn
Yang Liu, Ph.D
E-mail address: liuyang_leon@scu.edu.cn
Jianshu Li, Ph.D
E-mail address: jianshu_li@scu.edu.cn

S1. Materials and methods

S1.1. Materials

SN_A6 (DDDEEKC sequences, also abbreviated as DC, M_n=852.8) was purchased from Shanghai Apeptide Co., Ltd (Shanghai, China). Amine (polyethylene glycol) Maleimide (Mal-PEG-NH_2, M_n=2000) was bought from Ponsure Biotechnology Co., Ltd (Shanghai, China). Glutaric anhydride (GA), triclosan (TCS), Dichlormethane (DCM), triethylamine (TEA), 1-Ethyl-3-(3-dimethylaminopropyl)-carbodiimide (EDCI), 1-Hydroxybenzotriazole (HOBT), 4-Dimethylaminopyridine (DMAP), ethyl ether, methanol, crystalline violet and other chemical solvents and reagents were provided by Chengdu Haihong Reagent Co., Ltd (Chengdu, China). Hydroxyapatite (HA) sheets (5 × 2 mm^2, 8 × 2 mm^2, 12 × 2 mm^2) were purchased from National Engineering Research Center for Biomaterials, Sichuan University (Chengdu, China). Bovine serum albumin (BSA), lysozyme (Ly), Phosphate buffered solution (PBS), penicillin, streptomycin and trypsin were commercially available from Chengdu Bosco Biotechnology Co., Ltd (Chengdu, China). Fluorescein isothiocyanate (FITC) was purchased from Beijing Solarbio Science & Technology Co., Ltd (Beijing, China). Cell Counting Kit-8 (CCK-8) was obtained from Apexbio Co., Ltd (USA). Fluorescein diacetate (FDA) was bought from Sigma (USA). BCA Protein Assay Kit, Propidium iodide (PI), 2-(4-Amidinophenyl)-6-indolecarbamidine dihydrochloride (DAPI) were obtained from Beyotime Biotechnology Co., Ltd (Shanghai, China). Brain heart infusion medium (BHI), nutrient agar, LIVE/DEAD™ BacLight™ Bacterial Viability Kit (L7012), Gibco™ alpha-Modified Eagle Medium (alpha-MEM), and Gibco™ fatal bovine serum (FBS) were purchased from Thermo Fisher Scientific Co., Ltd (USA). Lactic acid assay kit (E-BC-K044-M) was bought from Elabscience Biotechnology Co., Ltd (Wuhan, China). Ultrapure water fabricated from the Milli-Q (Elix™ Essential 5, Merck Millipore, France) was used in all experiments.

S1.2. Characterization

^1H NMR and molecular weights of synthetic products were examined by Bruker NMR spectrometry (400 MHz) and time-of-flight mass spectrometry (Bruker AUTOFLEX III). The FT-IR spectra were examined by Fourier transform attenuated total reflectance infrared spectroscopy (ATR-FTIR, Thermo Fisher Corp, USA) in the wavelength range of 600-4000 cm^{-1} with a resolution of 4 cm^{-1} and 64 scans. Conformation of peptides and conjugates was examined by circular dichroism (CD, Chirascan plus Applied photophysics, UK) and the secondary conformations of peptides were calculated by CDPro software. Zeta potential was measured using a zeta potential meter (Zetasizer μV Malvern, UK). The elemental and chemical compositions of the surface were performed on an X-ray photoelectron spectrometer (Thermo Scientific K-Alpha$^+$, USA) from 0 eV to 1200 eV. The water contact angle was carried out using a DSA 25 contact angle goniometer (The droplet volume is 2 μL, KRUSS, Germany). Surface morphology, roughness and adhesion of proteins and bacteria were observed by scanning electron microscope (SEM, FEI/INSPECT F50, USA), Confocal Laser Scanning Microscope (CLSM, LSM 700, ZEISS, Germany) and fluorescence microscopy (IX71S1F-3, OLYMPUS, Japan), respectively. The fluorescence intensity of proteins and bacteria on surfaces was analyzed using ImageJ.

S1.3. Synthesis of GA-TCS (GT)

The peptide-polymer conjugate DPT was synthesized as illustrated in Figure 1a. Firstly, GA-TCS (GT) was synthesized according to literature [1]. Briefly, GA (6 mmol, 684 mg) was dissolved in DCM (20 mL) along with DMAP (0.13 mmol, 16 mg). TCS (4 mmol, 1158 mg) was then added, and the reaction was allowed to proceed at room temperature for 24 h. After rotary evaporation of the solvent, the crude product was subjected to column chromatography using the mixture of DCM and MeOH (DCM:MeOH=20:1, v/v) as the eluent to obtain GT. ^{1}H NMR spectrum of GT (400 MHz, $CDCl_3$) is shown in Figure S1: δ = 7.45 (d, J = 2.5 Hz, 1H), 7.20 - 7.16 (m, 3H), 6.85 (dd, J = 11.0, 8.7 Hz, 2H), 2.60 (t, J = 7.3 Hz, 2H), 2.44 (d, J = 7.2 Hz, 2H), 1.99 (t, J = 7.2 Hz, 2H). High-resolution mass spectrometry (Figure S2) confirmed the molecular weight of GT as $[M+H]^-$=403.301 (calculated GT: 403.64).

S1.4. Synthesis of Mal-PEG-TCS (PT)

Firstly, GT (0.1 mmol, 40.3 mg) was dissolved in anhydrous DCM (10 mL) under ambient conditions. Subsequently, triethylamine (0.3 mmol, 42 μL), EDCI (0.11 mmol, 21.2 mg) and HOBT (0.11 mmol, 14.86 mg) were added to the mixture to activate carboxy groups for 1 h at 0℃. Mal-PEG-NH_2 (0.1 mmol, 200 mg) was injected into the mixture and reacted overnight at room temperature. Finally, the crude product was precipitated in ice ether, centrifuged at 10000 rpm (**11180×g) and dried under vacuum to obtain Mal-PEG-TCS (PT). NMR spectrum is shown in Figure 1b: ^{1}H NMR of PT (400 MHz, $CDCl_3$) δ = 7.46 (d, J = 2.5 Hz, 1H), 7.17 (dd, J = 13.0, 6.6 Hz, 3H), 6.88 (d, J = 8.8 Hz, 1H), 6.82 (d, J = 8.7 Hz, 1H), 3.64-3.42 (m, 181H).

S1.5. Synthesis of DC-PEG-TCS (DPT)

The synthesis of DC-PEG (DP) and DPT was carried out as depicted in Figure S3a and Figure 1a. In brief, PEG (0.05 mmol, 100 mg) or PT (0.08 mmol, 120 mg) was dissolved in deoxygenated PBS (3 mL) and stirred. Then, PBS (2 mL) containing DC (0.075 mmol, 64 mg) was slowly added to the reaction tube and mixed uniformly. The reaction was carried out at room temperature for 24 h. After dialysis, DP and DPT were obtained by freeze-drying. ^{1}H NMR and TOF spectrum of DP are consistent with our previous studies (Figure S3)[28]. ^{1}H NMR spectrum of DPT (400 MHz, DMSO-d6) was shown in Figure 1b: δ = 8.70 (s, 1H), 8.36-7.71 (m, 26H), 7.51 (dd, J = 10.0, 5.5 Hz, 2H), 7.38 (ddd, J = 8.9, 5.7, 2.0 Hz, 2H), 7.11 (d, J = 8.8 Hz, 1H), 6.96 (d, J = 8.8 Hz, 1H), 3.54-3.36 (m, 985H).

S1.6. Antimicrobial activity of PT and DPT

The minimal inhibit concentration (MIC) and minimum bactericidal concentration (MBC) of PT and DPT were tested following the standardized guidelines established by the Clinical and Laboratory Standards Institute (CLSI) [2, 3]. A series of two-fold dilutions of PT and DPT were prepared in 96-well plates (100 μL/well), followed by the addition of 100 μL of bacterial suspension (1 × 10^6 CFU mL^{-1}) to achieve a final volume of 200 μL per well. The pure medium and bacterial solution were included as the blank and control group, respectively. Then, the plates were incubated anaerobically at 37°C for 24 h and the bactericidal rate (B%) was calculated using the following Equation (1):

$$\mathrm{B}(\%) = \frac{ODcontrol - ODtest}{ODcontrol - ODblank} \times 100 \quad (1)$$

Where ODcontrol, ODtest and ODblank represent the absorbance of bacteria control group, the experimental group and the BHI medium group at 600 nm, respectively. All measurements were performed in triplicate.

Subsequently, the antibacterial activity was further evaluated using live/dead bacterial staining assays. Briefly, all samples (1 × MIC) were co-cultured with bacteria for 24 h and then gently washed three times with physiological saline. A cocktail of SYTO 9 and propidium iodide was subsequently introduce and allowed to incubate for 15 min under ambient temperature in complete darkness. The samples were then subjected to confocal microscopy imaging.

S1.7. Investigation of anti-biofilm activity

S1.7.1. Inhibition of biofilm formation

To assess the anti-biofilm activity of DPT, 50 μL of sterile saliva was initially introduced to 96-well plates and incubated at 37°C for 2 hours to establish salivary pellicles, thereby replicating the physiological conditions of pellicle-coated tooth surfaces. The experimental protocols received ethical approval from the Institutional Review Board of West China Hospital, Sichuan University (Approval No.: WCHSIRB-CT-2020-439). Afterwards, 190 μL of a mixture of different concentrations of DPT and BHI containing 1% sucrose was added to a saliva-coated 96-well plate. Then 10 μL of *S. mutans* suspension with OD=0.6 was added and incubated at 37°C for 24 h under anaerobic conditions to detect the minimum anti-biofilm concentration using Equation (1). Bacteria treated for 24 h with the aforementioned concentrations of PEG, DC, DP, and DPT were combined with a dye cocktail containing SYTO 9 and propidium iodide, followed by incubation at room temperature in the dark for 15 min. Following treatment, the microbial samples were analyzed using laser confocal fluorescence microscopy, with quantitative fluorescence intensity measurements obtained through ImageJ software analysis. For the crystal violet biofilm quantification assay, the microplate wells were gently rinsed three times with normal saline to remove non-adherent cells. Subsequently, adherent biofilms were fixed with methanol for 15 min at room temperature and stained with 1% (w/v) crystal violet solution for 15 min. Following five consecutive PBS washes to eliminate unbound dye, the absorbed crystal violet was solubilized in 30% (v/v) glacial acetic acid through 30-minute incubation at 37°C. The optical density of the dissolved stain was quantitatively measured at 600 nm using a microplate spectrophotometer with appropriate blank corrections [4].

S1.7.2. Biofilm removal assay

Briefly, *S. mutans* biofilms were first inoculated in saliva-coated 48-well plates with 10 μL of *S. mutans* (OD_{600}=0.6) in 1 mL BHI containing 1% sucrose at 37 °C overnight anaerobically, followed by the addition of the same concentrations of PEG, DC, DP and DPT as described in section 2.9.1 for a continued anaerobic incubation of 24 h. The biofilm removal ability was evaluated by live/dead staining and crystalline violet staining.

S1.7.3. Investigation of the lactate production and biofilm-related gene *expressions*

In order to investigate the anti-biofilm mechanism of DPT (0.15 mM), the supernatant and precipitates of *S. mutans* biofilms obtained in *S1.7.2.* were collected by centrifugation (10000 rpm, ***11180×g, 5 min). The lactate concentrations of the *S. mutans* supernatant was measured using a lactic acid assay kit, and the expression levels of *S. mutans* biofilm-related genes were measured by qRT-PCR [5].

S1.7.4. Evaluation of anti-biofilm activity on HA disks

To assess the anti-biofilm activity of DPT *in vitro*, an oral biofilm model was established on the surface of HA disks. Briefly, HA disks were first soaked in sterile saliva supernatant at 37°C for 2 h in 24-well plates. Subsequently, each of these HA disks was inoculated with 10 μL of *S. mutans* (OD = 0.6) in 1 mL of BHI containing 1% sucrose at 37°C overnight anaerobically. Meanwhile, DC, DP and DPT (0.15 mM) were added respectively for comparison. The ability to inhibit biofilm formation was evaluated using live/dead staining and crystalline violet staining, and the corresponding bacterial morphology was examined by SEM.

In addition, *S. mutans* biofilms were similarly constructed on the surface of HA as described in section *S1.7.2*. Then 0.15 mM DC, DP and DPT was added respectively for a further incubation of 24 h. The ability to remove biofilms *in vitro* was evaluated using live/dead staining, crystalline violet staining as well as SEM.

S1.8. Saturation adsorption and targeting capacity of DPT

The saturation adsorption of DPT was quantified using previous methods[6], and the obtained saturation concentration was utilized for the subsequent preparation and characterization of multifunctional coatings. FITC-DPT was also synthesized to qualitatively validate its targeting performance on bovine dental slices. First, solutions of PEG, DC, DP and DPT (5 mg mL^{-1}) were prepared in 0.1 M carbonate buffer (pH 9.0). Separately, FITC was dissolved in DMSO (1 mg mL^{-1}) and then slowly added to the stirring peptide solution at a 1:10 molar ratio (FITC : peptide) using a syringe. After 24 h of reaction, the mixture was dialyzed for three days until the dialysis water became colorless, then freeze-dried and stored at 4°C in the dark. For adsorption experiments, bovine dental slices were placed in a 24-well plate, and 1 mL of the prepared solutions (1 mg mL^{-1}) was added to each well for 1 h. The slices were then rinsed three times with ultrapure water and analyzed using confocal laser scanning microscopy (CLSM) with an excitation wavelength of 488 nm.

S1.9. Anti-fouling performance

The coated dental slices were equilibration by fresh PBS for 1 h at room temperature in 24-well plate, then 1 mL of BSA and lysozyme solution (2 mg mL^{-1}) was added and incubated at 37°C for 2 h. The slices were then washed three times with a gentle rinse to remove unadhered proteins and soaked in 200 μL SDS (2 wt%) aqueous solution at 37°C for 20 min to extract adsorbed proteins from surfaces. Quantitative analysis of adsorbed proteins on the surfaces was detected using the Micro BCA™ Protein Assay Kit. To more visually detect the anti-protein adhesion capacity of the surfaces, 1 mg mL^{-1} FITC-labelled BSA and Ly solutions were incubated with the coated dental slices under the same conditions for 2 h at 37℃. After gently rinsed three times with PBS, the proteins on the surface were observed with CLSM.

All coated dental slices were incubated in BHI medium containing *S. mutans* (10^6 CFU mL^{-1}) for 4 h. After that, the bacterial suspension was removed and the slices were washed three times with sterile PBS. The bacteria on surfaces were dyed by LIVE/DEAD™ Viability Kit for 15 min in the dark, rinsed with sterile PBS for three times and then imaged by CLSM. Subsequently, the tooth slices were fixed overnight at 4°C in 2.5% w/v glutaraldehyde, dehydrated in graded concentrations of ethanol (25%, 50%, 75%, 90%, 100%) for 15 min in sequence, then dried and sprayed with gold to observe bacterial morphology by SEM.

S1.10. Biocompatibility *in vitro*

Human Oral Keratinocytes (HOK) were used to assay the cytotoxicity of different concentrations of PEG, DC, DP and DPT and the corresponding coatings. Briefly, 2 × 10^4 HOK cells/well were inoculated in 48-well plates and incubated at 37℃ for 24 h under a 5% CO_2 atmosphere. The sterilized dental slices coatings were inverted on the cells and co-cultured for 24 h and 72 h. After co-cultured with CCK-8 reagents for 3 h, the absorbance at 450 nm was measured using a microplate spectrophotometer. The cell viability (%) was calculated using Equation (2):

$$\text{Cell viability}(\%) = \frac{ODtest - ODblank}{\text{ODcontrol} - \text{ODblank}} \times 100 \quad (2)$$

Where ODcontrol, ODtest and ODblank was the absorbance of blank dental slices group, experimental group, pure CCK-8 group at 450 nm, respectively.

To further evaluate the cell viability, HOK cells were incubated with the mixtures of 10 μg mL^{-1} FDA and 1 μg mL^{-1} PI solutions at 37°C for 10 min in darkness after 24 h and 72 h, and then quickly observed under fluorescence microscopy. Finally, the cell morphology was imaged after the nuclei and F-actin of cells were stained by DAPI and Rhodamine-labeled Phalloidin, respectively.

In addition, the hemocompatibility of different concentrations of PEG, DC, DP and DPT as well as corresponding coatings was evaluated. Briefly, all samples were incubated with 1 mL 2% whole blood which was diluted with normal saline. After incubation for 2 h at 37℃, centrifugation was performed at 5000 rpm for 5 min, and the supernatant was measured at a wavelength of 540 nm using a microplate reader. The hemolysis ratio was calculated using Equation (3):

$$\text{Hemolysis ratio}\ (\%) = \frac{A - B}{C - B} \times 100 \quad (3)$$

Where *A*, *B*, *C* was the absorbance of the experimental group, negative group, and positive group respectively. The negative and positive groups were 2% whole blood diluted with normal saline and reverses osmosis (RO) water, respectively.

S1.11. Stability of the coatings

To assess the stability of the functional coatings in oral, the coatings prepared with FITC-labelled peptides and peptide-polymer conjugates were immersed in saliva supernatant for 12 h at 37°C, respectively. The surface fluorescence, antimicrobial properties and wettability were examined.

S1.12. Anti-calcification properties and molecular simulation

The ability of DPT to inhibit spontaneous crystalline precipitation of calcium phosphate was evaluated according to references [7-9]. Briefly, $CaCl_2$ (10 mmol) solutions containing 2 mg mL^{-1} PEG, TCS, DC and DPT were first prepared individually. Subsequently the same volume of Na_2HPO_4 solution (6 mmol) was gradually added dropwise to obtain supersaturated composite mineral solutions. The particle size and surface morphology of minerals in solution were examined. The composite mineral solutions were freeze-dried to obtain different composite nanoparticles and their phase composition and crystal structure were examined by FTIR, XRD and TEM.

In order to simulate the formation process of oral calculus, the anti-calcification ability of DPT-modified dental slices was tested using a rapid mineralization method with minor modification by attaching bacteria before mineralization and adding bacterial suspension directly to the mineralizing solution (50 mM $CaCl_2$, 30 mM NaH_2PO_4). Briefly: (1) all dental slices were incubated in BHI medium

containing *S. mutans* (1×10^6 CFU mL^{-1}) for 12 h. The unadhered bacteria were then gently rinsed away and slices were mineralized by immersion in a mineralizing solution. After that, surface mineral formation was examined by SEM. (2) A suspension of *S. mutans* was first added to the mineralizing solutions to a final concentration of 1×10^6 CFU mL^{-1}. The bare and DPT-modified dental slices were subsequently immersed for mineralization and the surface mineral formation was examined by SEM.

Molecular simulation: We carried out all the simulations using the GROMACS 2021 software [10]. The DPT polymers were simulated using CHARMM general force field [11] and the rests using CHARMM 36 force field [12, 13]. The molecular dynamics simulations employed a Langevin integrator to maintain the system temperature at 298 K. Lennard-Jones interactions were gradually attenuated between 10-12 Å using a force-based switching function, while long-range electrostatic interactions were computed through the particle-mesh Ewald (PME) method [14] with a precision tolerance of 1×10^{-5}. Force field parameters for hydroxyapatite (HA), phosphate ions (PO_4^{3-}), and calcium ions (Ca^{2+}) were derived from established literature [15]. The simulation system contained 78 diphosphate groups (DPTs), 593 phosphate ions, 378 calcium ions, and a HA (001) facet substrate within an aqueous environment (10.3 nm × 10.3 nm × 12.0 nm), with the substrate surface maintained at pH 5. During the equilibration phase (30 ns), the X-Y dimensions were constrained through zero compressibility settings, while Z-axis pressure control (1 bar) was achieved via the Parrinello-Rahman barostat using a 1-fs timestep [16]. Subsequent production runs implemented NVT ensemble conditions with a 2-fs timestep for 200 ns, continuing until dimensional stability in the Z-axis was confirmed.

S1.13. Dental plaque control *in vivo*

The animal experiments conducted in this study were approved by the Animal Research Ethics Committee of Sichuan University (Approval No. KS2023370), in accordance with national regulations on laboratory animal welfare and institutional ethical review protocols. Male Sprague Dawley rats (SD strain, aged 8 weeks) were utilized for the *in vivo* experiments. Bovine tooth slices were sharpened into 6 × 5 mm^2 plates by grinding with a pregrinder, and then holes (d = 0.6 mm) were punched on both sides of them with an electric drill to facilitate fixation in the mouths of SD rats according to the reference [17]. The SD rats were randomly allocated into three experimental groups: Control, CHX, and DPT, with each group consisting of five animals. Following isoflurane anesthesia, the three groups of dental slices were surgically secured within the oral cavities of SD rats using sutures, ensuring complete exposure of the teeth to native saliva. Following surgical fixation of the dental slices in the oral cavity, all experimental subjects received daily inoculation with a *S. mutans* suspension (1×10^8 CFU mL^{-1}) for three consecutive days, accompanied by ad libitum access to 5% sucrose-supplemented drinking water throughout the experimental period. From day 4 onwards, experimental groups received twice-daily administration of ultrapure water (Control), commercially available chlorhexidine gluconate mouthwash (CHX), and DPT solution (0.5 mg mL^{-1}), respectively. A liquid diet was applied throughout to prevent dislodgement of the dental slices. After five days of treatment, the dental slices and saliva were collected and then investigated by bacterial live/dead staining, SEM and flora analysis. In addition, oral and tongue mucosal specimens were collected from all experimental groups and subsequently subjected to hematoxylin and eosin (H&E) staining for histological assessment of biocompatibility. The oral antimicrobial capacity of each group was also examined by ultrasonically separating the bacteria on the dental slices to smear

agar plates. Finally, to assess systemic biocompatibility and biosafety, complete blood count analysis and hematoxylin-eosin (H&E) staining were conducted on cardiac, hepatic, splenic, and renal tissue sections obtained from Sprague-Dawley (SD) rats.

S1.14. Statistical analysis

Statistical analysis was performed using one-way ANOVA. Quantitative data are presented as mean ± standard deviation, with statistical significance thresholds defined as *p<0.05 and **p<0.01.

Supplementary Figures

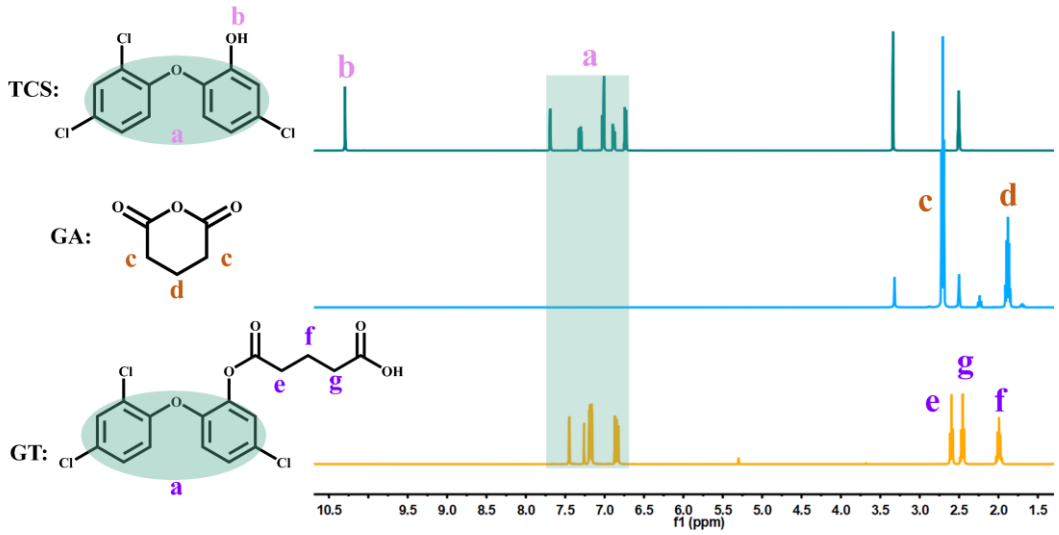

Figure S1. ^{1}H NMR spectra of TCS, GA and GT.

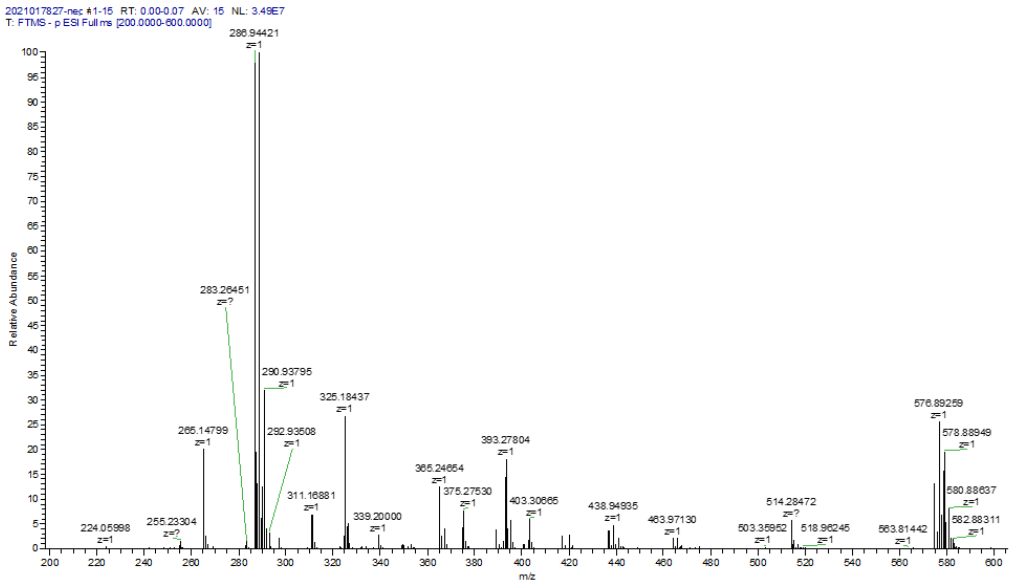

Figure S2. HRMS spectrum of GT.

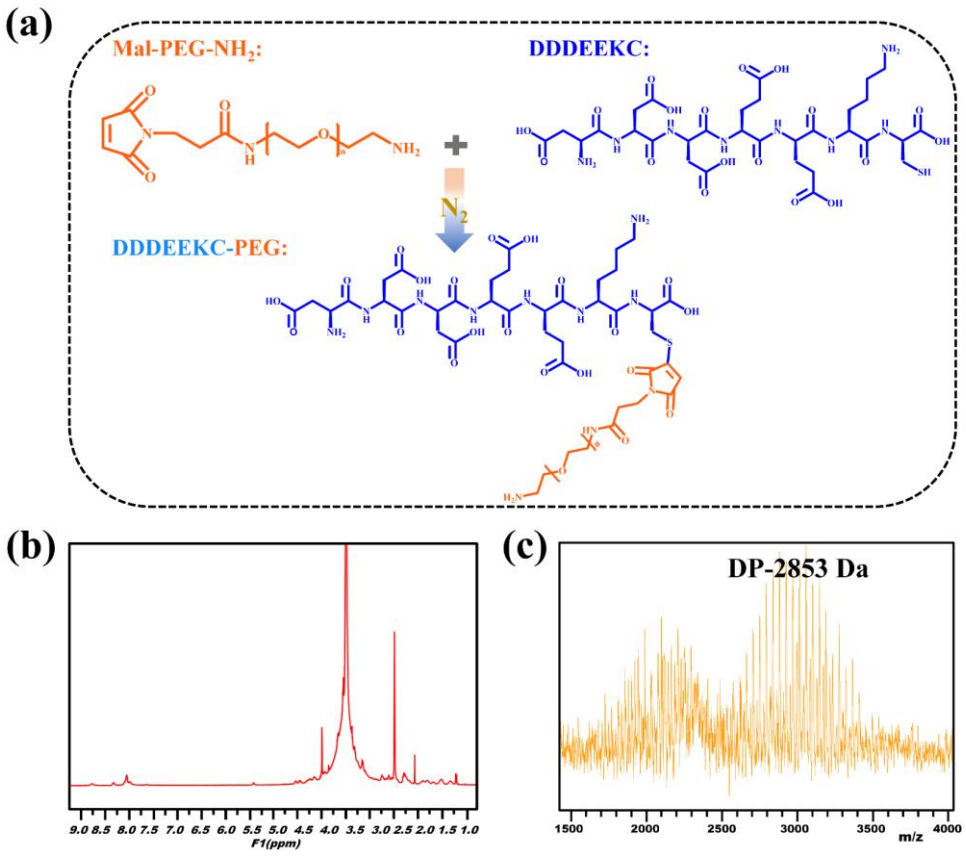

Figure S3. (a) The synthesis route of the peptide-polymer conjugate DP. (b) ^{1}H NMR spectrum of DP in DMSO-d6. (c) Time-of-flight mass spectra of DP.

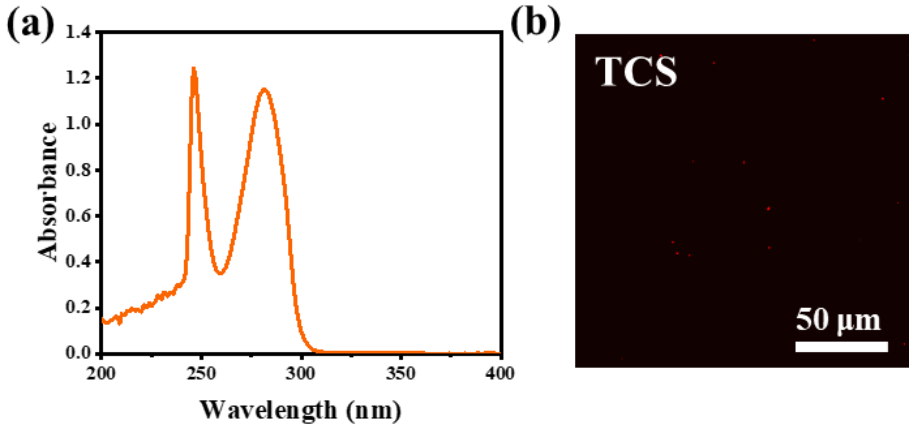

Figure S4. (a) UV-vis spectrum of TCS in blended solvents (MeOH/water=1:1). (b) Fluorescent images of *S. mutans* incubated with 0.15 mM of TCS.

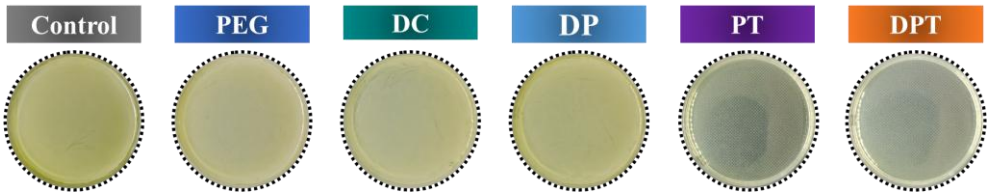

Figure S5. Photographs of *S. mutans* colonies after various treatments for 24 h without dilution.

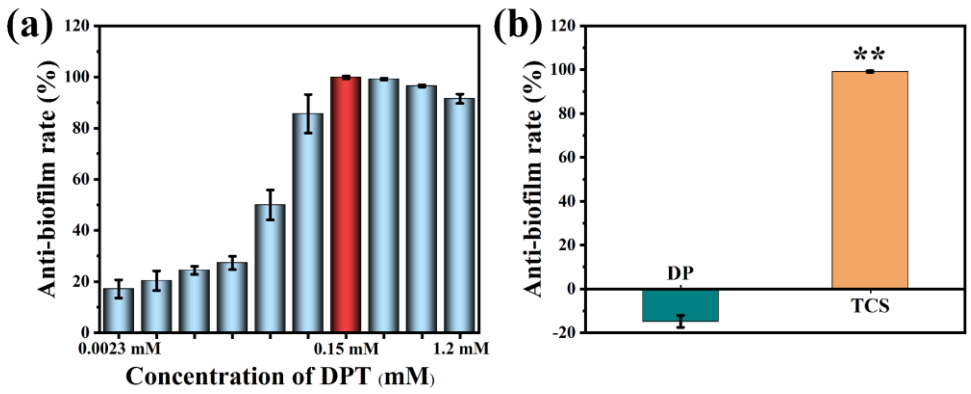

Figure S6. Biofilm inhibition assay of DPT. (a) Inhibition of biofilm formation capacity in different concentrations of DPT. (b) The ability to inhibit biofilm formation of 0.15 mM DP and TCS.

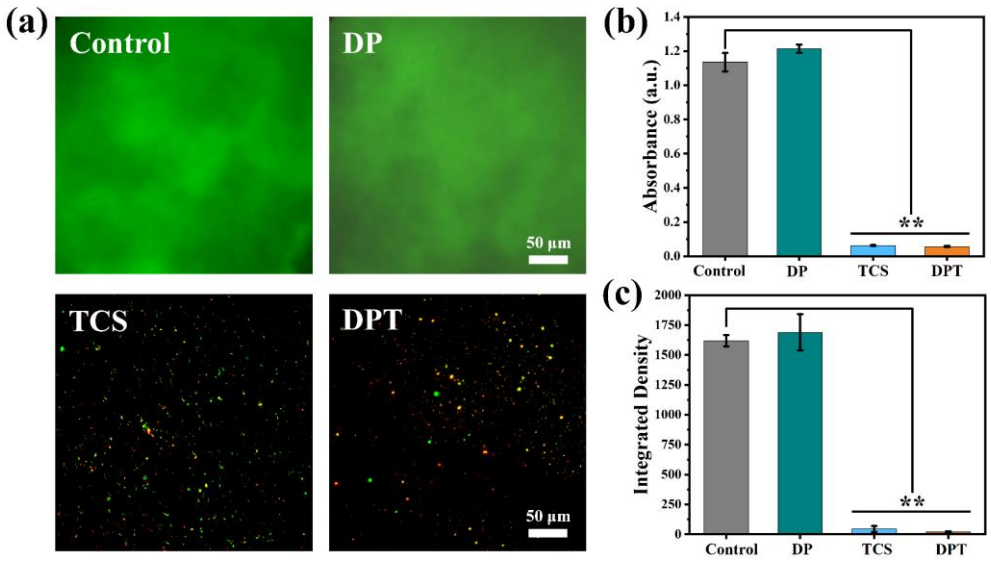

Figure S7. Biofilm formation inhibition assay. (a) Fluorescence images of live/dead staining of biofilms, (b) fluorescence intensity and (c) the absorbance of crystalline violet staining after treatment with 0.15 mM DP, TCS and DPT respectively.

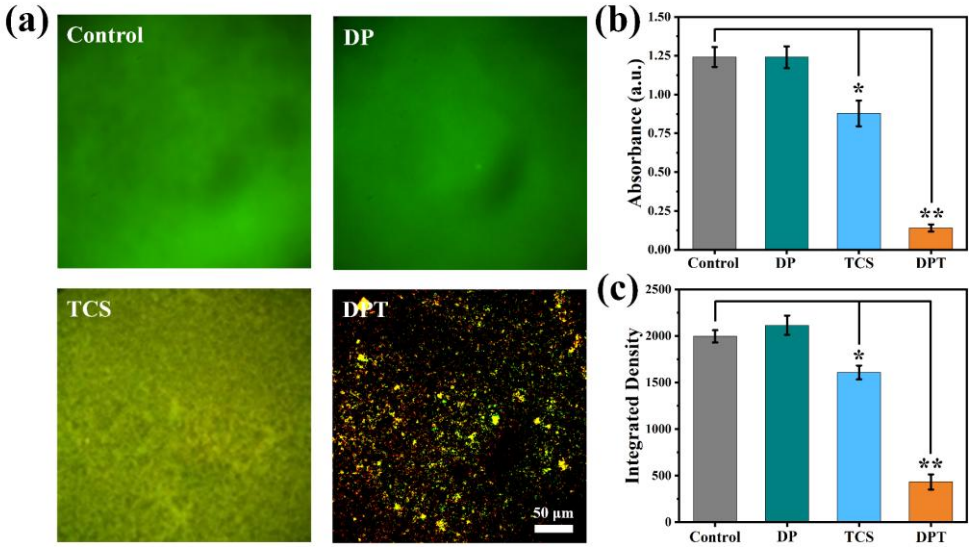

Figure S8. Biofilm clearance activity. (a) Fluorescence images of live/dead staining of biofilms, (b) fluorescence intensity and (c) the absorbance of crystalline violet staining after treatment with 0.15 mM DP, TCS and DPT, respectively.

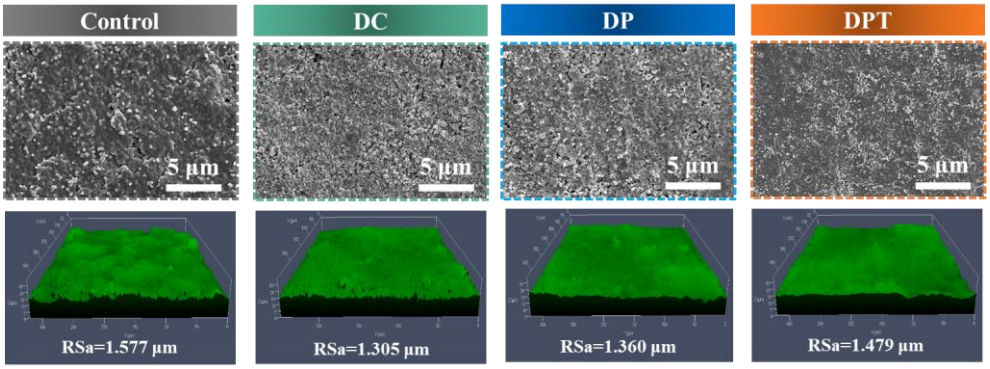

Figure S9. SEM and CLSM images of untreated and DC, DP, DPT-treated HA slides.

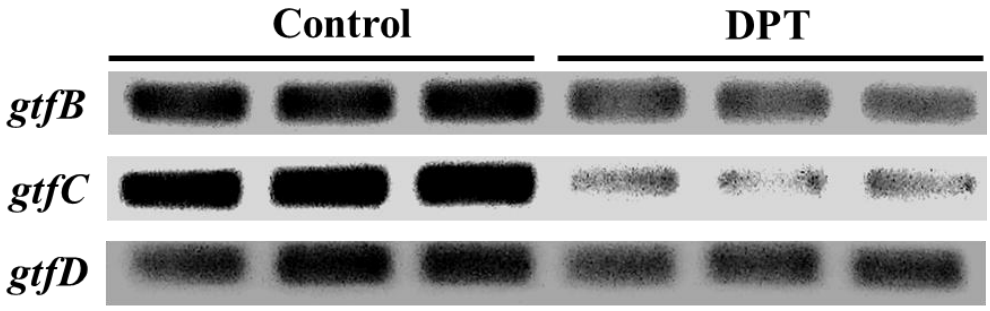

Figure S10. Agarose gel electropherogram of *gtfB*, *gtfC*, *gtfD* gene.

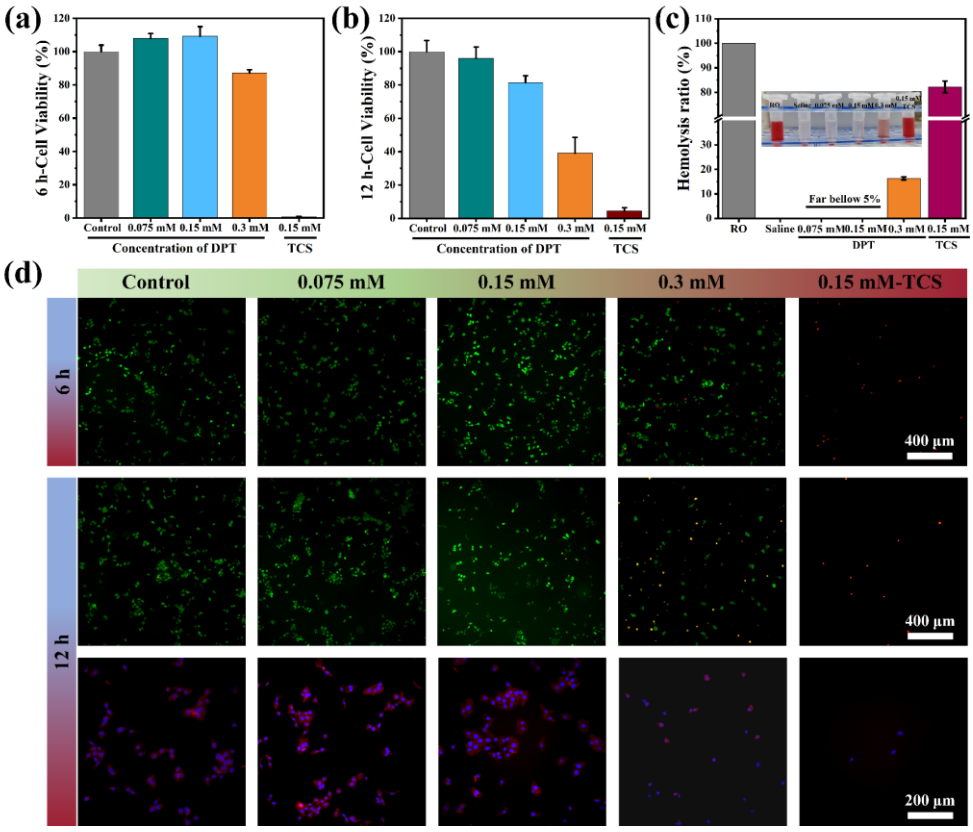

Figure S11. HOK Cell viability after co-incubation of DPT at different concentrations for (a) 6 h and (b) 12 h. (c) Hemolysis ratio of different concentrations of DPT and 0.15 mM TCS. (d) Fluorescence images of live/dead staining and morphological staining after co-incubation of DPT at different concentrations for 6 h and 12 h.

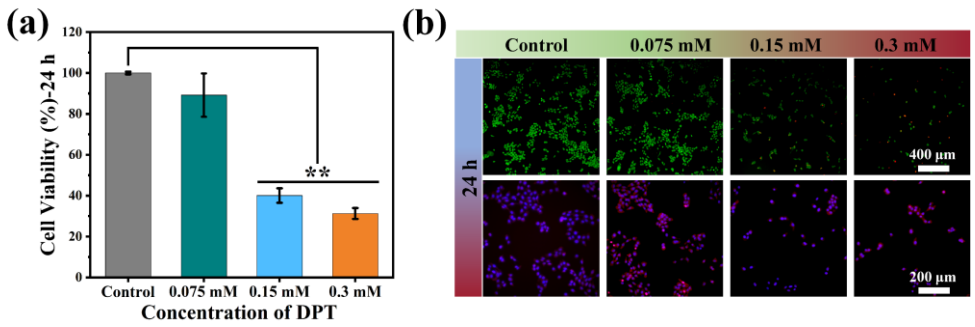

Figure S12. (a) HOK Cell viability after co-incubation of DPT at different concentrations for 24 h. (b) Fluorescence images of live/dead staining and morphological staining after co-incubation of DPT at different concentrations for 24 h.

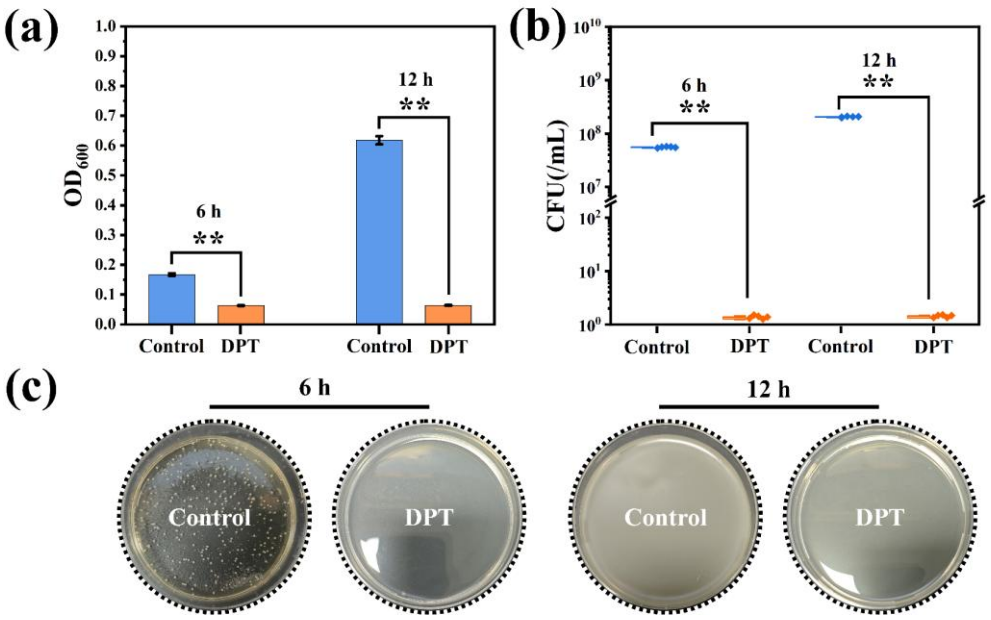

Figure S13. (a) OD_{600} values and (b) quantified CFU of *S. mutans* after co-incubation with DPT for 6 h and 12 h. (c) Photographs of *S. mutans* colonies after treated with DPT for 6 h and 12 h.

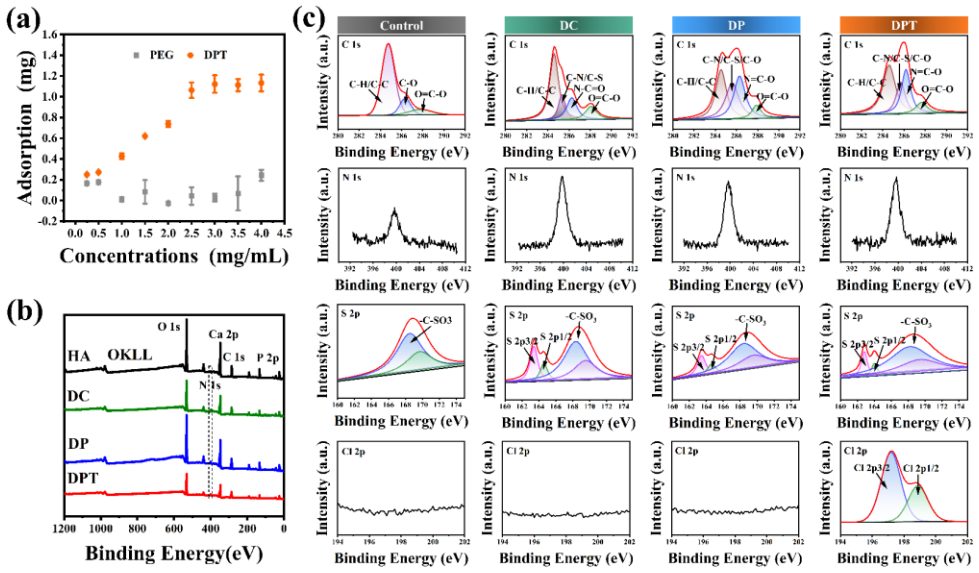

Figure S14. Saturation adsorption capacity and characterization of coatings. (a) Comparative analysis of saturation adsorption levels between DPT and PEG. (b) XPS wide scan spectra and (c) C 1s, N 1s, S 2p and Cl 2p high-resolution spectra of bare HA, DC, DP and DPT coating, respectively.

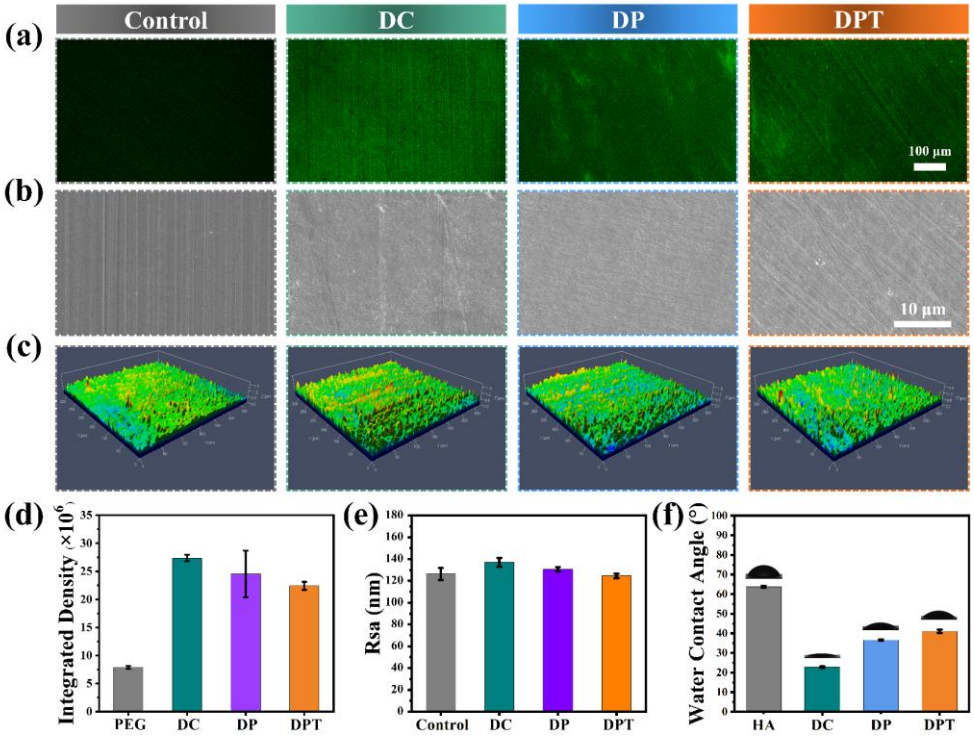

Figure S15. Targeting efficiency evaluation and characterization of coatings. (a) Fluorescence microscopy visualization of FITC-labeled PEG, DC, DP, and DPT distribution patterns on dental substrates after adsorption. (b) SEM and (c) CLSM images of the surfaces of blank dental slices, DC, DP and DPT coating, respectively. (d) The fluorescence intensity of FITC labelled PEG, DC, DP and DPT coating on dental slices. (e) Surface roughness of PEG, DC, DP and DPT coating on dental slices. (f) Water contact angle (WCA) measurements for blank HA sheets, DC, DP, and DPT coatings.

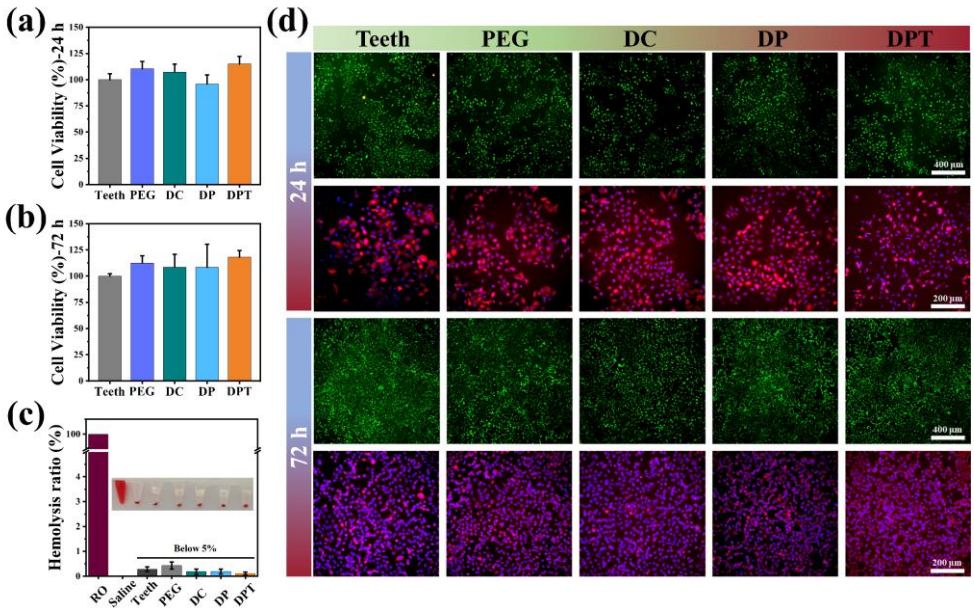

Figure S16. Biocompatibility evaluation of different coatings *in vitro*. (a) 24 h and (b) 72 h HOK cell viability assays on blank dental slice and DC, DP, DPT coatings, respectively. (c) Hemolysis ratio and representative images comparing blank dental slice and DC, DP, DPT coating. (d) Fluorescence microscopy images of Live/dead staining and morphological staining of HOK cells incubated after 24 h and 72 h.

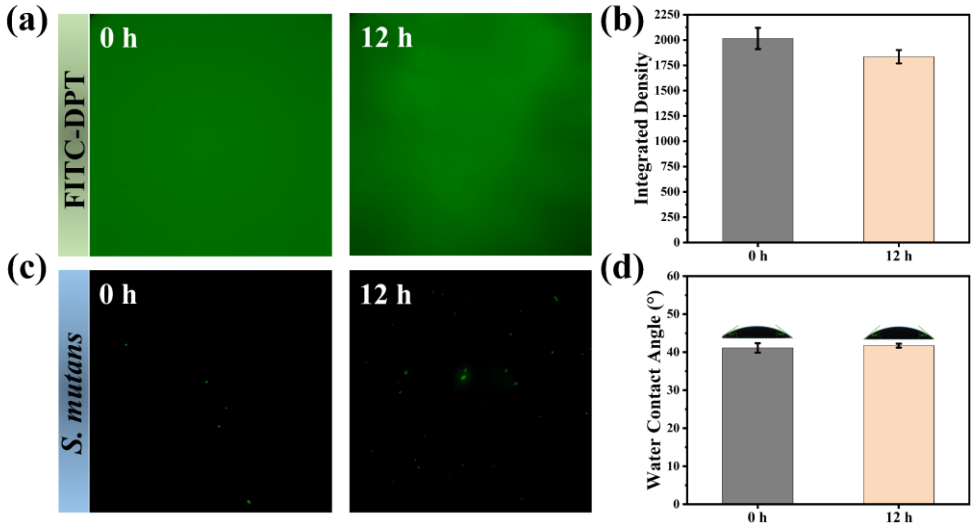

Figure S17. Stability of the DPT coating in the oral cavity. (a) The surface fluorescence of FITC-DPT coating, (c) adhesion of *S. mutans*, (b) the antibacterial properties and (d) water contact angle of DPT coating before and after immersion in human saliva supernatant for 12 h at 37℃.

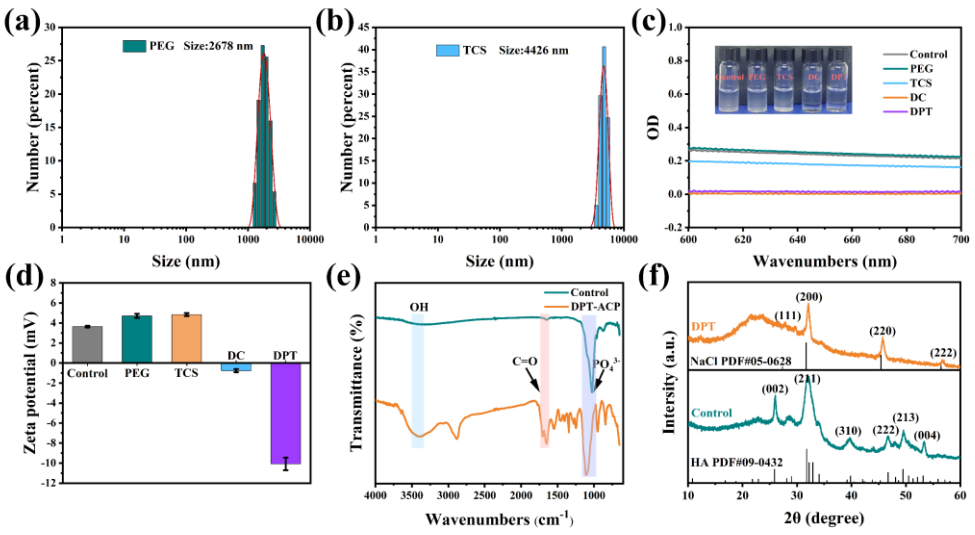

Figure S18. Dynamic light scattering of nanocomposites in (a) PEG and (b) TCS groups. (c) The turbidity and (d) zeta potential of nanocomposites in control, PEG, TCS, DC and DPT groups. (e) Infrared spectra and (f) XRD pattern of nanocomposites in Control and DPT groups.

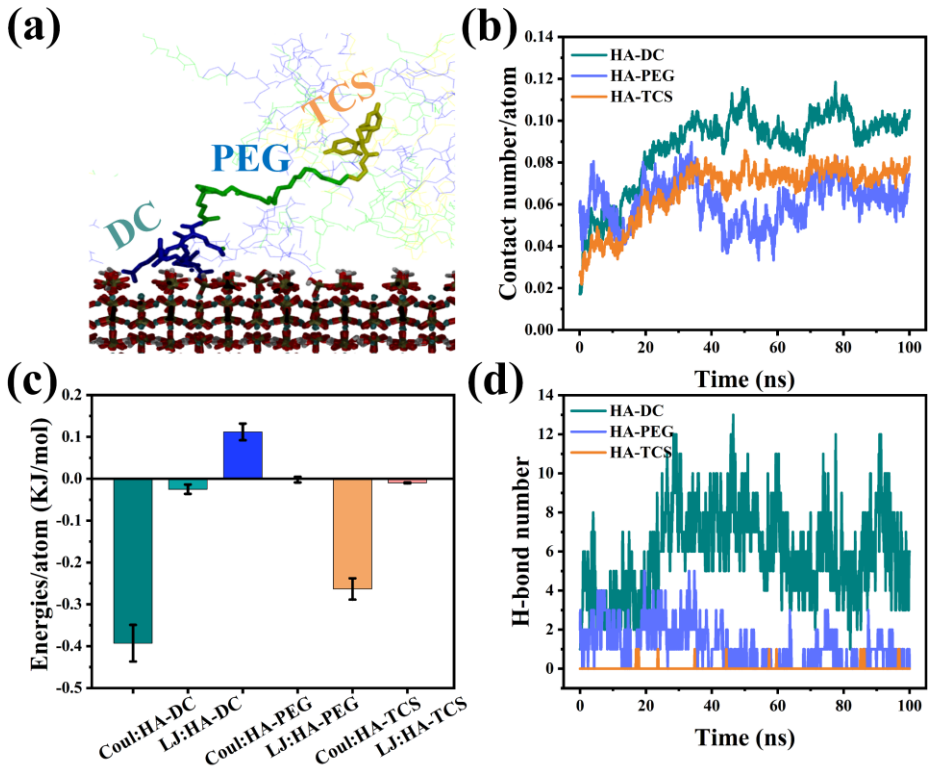

Figure S19. Molecular dynamics (MD) simulations of random distributed DPT polymers assembled to HA surface. DC, PEG and TCS were considered separately. (a) The simulation snapshot at the end of the simulation (Water is not shown for clarity). (b) The contact numbers, (c) coulombic and Lennard-Jones (LJ) energies and (d) hydrogen bond numbers of different DPT components with HA. Contact numbers and energies were normalized by the atom numbers in each DPT component.

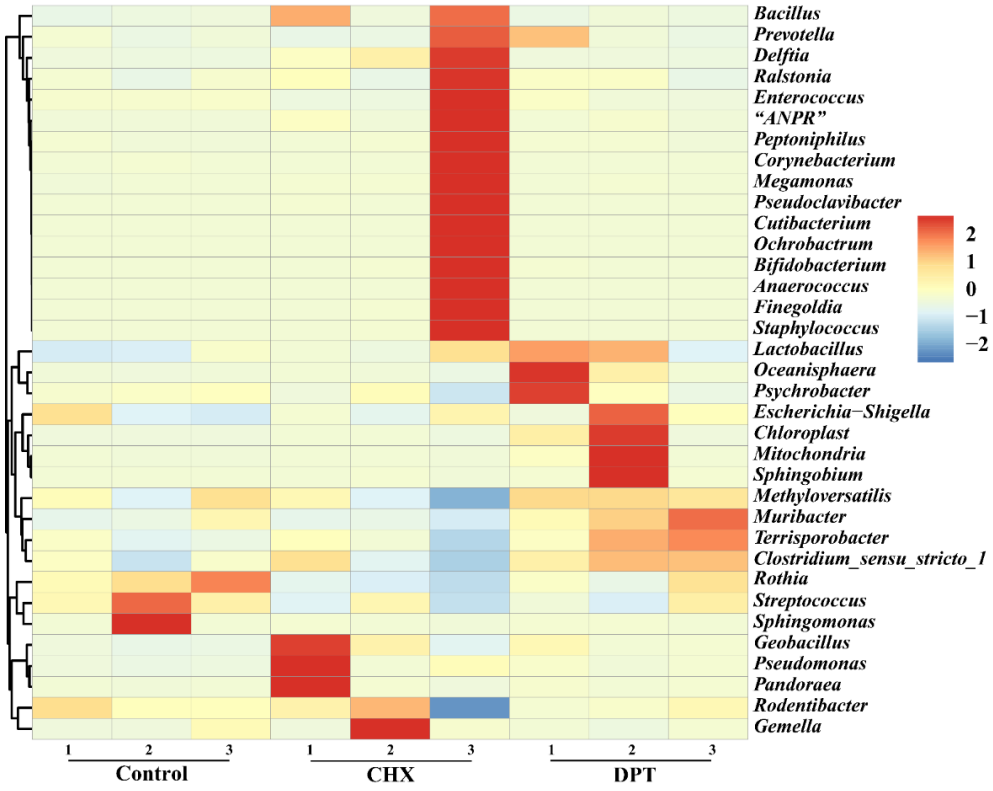

Figure S20. The heatmap of relative abundance of community in rat mouth of each sample.

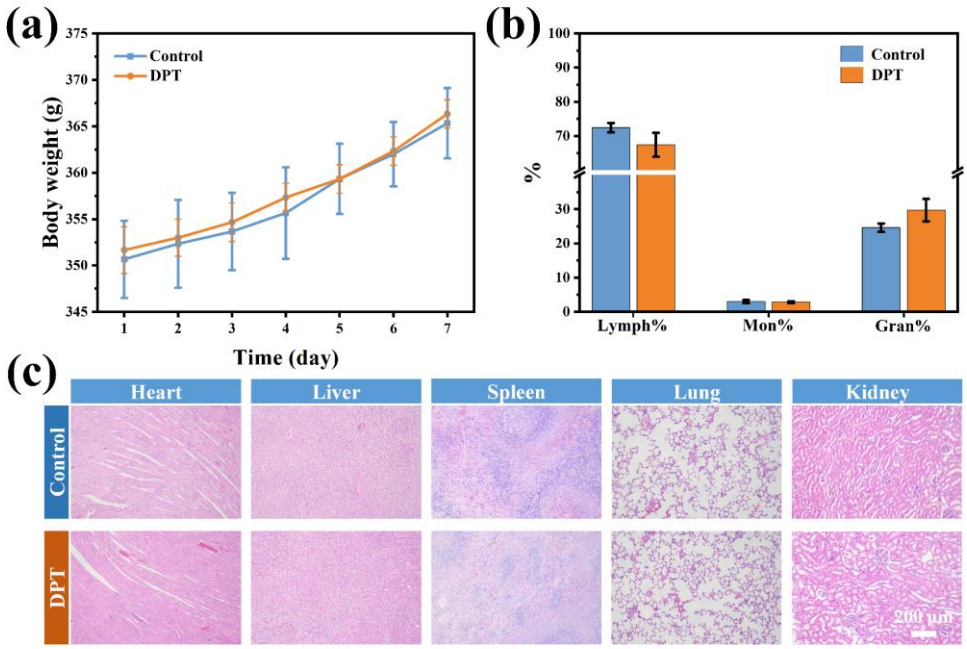

Figure S21. Biosafety evaluation in vivo. (a) The body weight variation of mice in Control and DPT gavage groups. (b) The blood routine analysis of rats in each group (% represents the relative proportion of neutrophils, lymphocytes, and monocytes). (c) H&E staining images of heart, liver, spleen, lung, and kidney of rats in each group. Data are means ± s.d. (n = 3). *p <0.05, **p < 0.01.

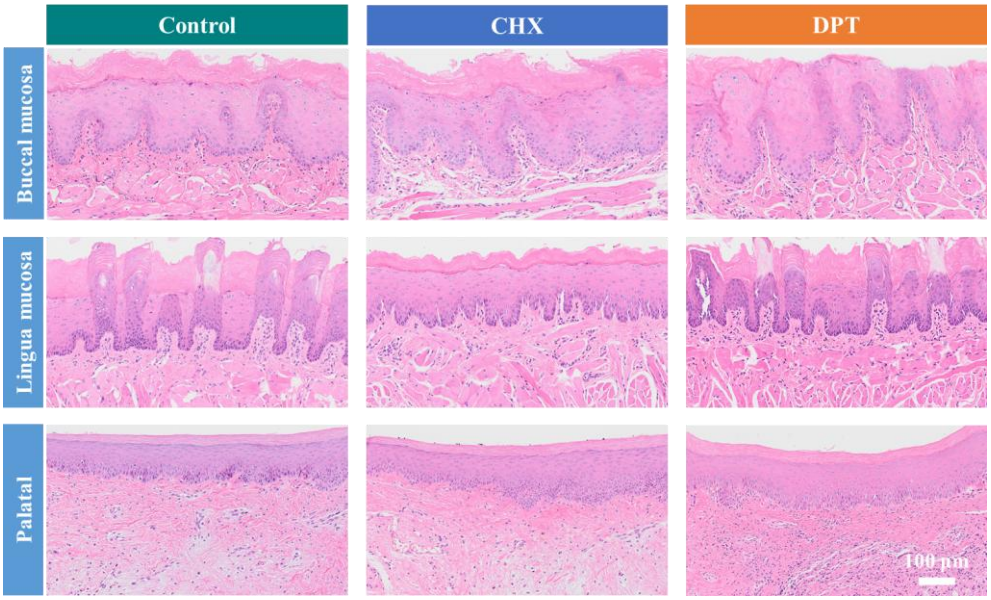

Figure S22. H&E staining of the buccal mucosa, lingua mucosa and palatal of rats in each group.

Supplementary Tables

Table S1. The MIC and MBC of PT and DPT, respectively.

Sample	MIC (μg mL^{-1})	MBC (μg mL^{-1})
PT	62.5	125
DPT	62.5	125

Table S2. Ratio of secondary conformation composition of DC, DP and DPT.

Formulation	α-helix (%)	β-sheet (%)	β-turn (%)	Random coil (%)
DC	0	34.19	27.46	38.35
DP	2.62	33.07	26.77	37.54
DPT	0	36.10	26.93	36.97

Table S3. Primers used in quantitative real-time PCR for detecting *gtfB, gtfC, gtfD, srtA, nox, sodA* levels.

Target gene	Fp (5'to 3')	Rp (5'to 3')
gtfB	TGCTCCAAATTGCTGGGGAT	CGTTGTCACTCCATGCCTCT
gtfC	CGTCTGTCCGCTATGGTAAAG	GGTCAAGAGTAAAGGTCGGTAAG
gtfD	TGCAAGCGACGGAAAACAAG	GCCTGTCAGAGCTTCACCAT
srtA	TGGCAATTCCGCCAATTACAG	AAGGCTGCCCATTCTTCCTT
nox	CGCTCTTCGCTCAGGTATTGT	CGCTTTGCTTTTTCTTGCGTT
sodA	GCTCAGGTTGGGCTTGGTTA	AGCGTGTTCCCAGACATCAA
16S rRNA	CCTACGGGAGGCAGCAGTAG	CAACAGAGCTTTACGATCCGAAA

Table S4. The blood routine analysis of SD rats in the control and DPT groups.

Test items	Normal Range	Control	DPT
RBC [a)]	5.60-7.89 (10^{12}/L)	7.683 ± 0.175	8.477 ± 0.208
HGB [b)]	120-150 (g/L)	159.667 ± 3.055	172.667 ± 3.786
HCT [c)]	36.0-46.0 (%)	47.433 ± 1.15	49.967 ± 1.097
MCV [d)]	53-68.8 (fL)	61.8 ± 0.1	58.967 ± 0.153
MCH [e)]	16.0-23.1 (pg)	20.767 ± 0.115	20.333 ± 0.058
MCHC [f)]	300-341 (g/L)	336.333 ± 2.309	345 ± 1
RDW [g)]	11.0-15.5 (%)	14.467 ± 0.462	13.9 ± 0.458
WBC [h)]	2.9-15.3 (10^9/L)	19.6 ± 1.836	18.5 ± 1.058
Lymph# [i)]	2.6-13.5 (10^9/L)	14.233 ± 1.501	12.467 ± 0.709
Mon# [j)]	0.0-0.5 (10^9/L)	0.567 ± 0.058	0.533 ± 0.058
Gran# [k)]	0.4-3.2 (10^9/L)	4.8 ± 0.458	5.5 ± 0.781

[a)] RBC, red blood cell count; [b)] HGB, hemoglobin; [c)] HCT, hematocrit; [d)] MCV, mean corpusular volume; [e)] MCH, mean corpusular hemoglobin; [f)] MCHC, mean corpusular hemoglobin concerntration; [g)] RDW, red blood cell volume distribution width; [h)] WBC, white blood cell count; [i)] Lymph#, lymphocyte count; [j)] Mon#, monocyte count; [k)] Gran#, granulocyte.

References

[1] L. Yang, C. Zhang, F. Huang, J. Liu, Y. Zhang, C. Yang, C. Ren, L. Chu, B. Liu, J. Liu, *J. Controlled Release* **2020**, *324*, 354.

[2] J. He, R. Eckert, T. Pharm, M. D. Simanian, C. Hu, D. K. Yarbrough, F. Qi, M. H. Anderson, W. Shi, *Antimicrob. Agents Chemother.* **2007**, *51*, 1351.

[3] E. Isogai, H. Isogai, K. Takahashi, K. Okumura, P. Savage, *Oral Microbiol. Immunol.* **2009**, *24*, 170.

[4] J. Wang, X.-Y. Chen, Y. Zhao, Y. Yang, W. Wang, C. Wu, B. Yang, Z. Zhang, L. Zhang, Y. Liu, *ACS Nano* **2019**, *13*, 11686.

[5] M. Gu, S. Jiang, X. Xu, M. Y. Wu, C. Chen, Y. Yuan, Q. Chen, Y. Sun, L. Chen, C. Shen, *Adv. Sci.* **2022**, *9*, 2106071.

[6] Y. Liu, C. Ding, L. He, X. Yang, Y. Gou, X. Xu, Y. Liu, C. Zhao, J. Li, J. Li, *J. Mater. Chem. B* **2018**, *6*, 1984.

[7] J. He, J. Yang, M. Li, Y. Li, Y. Pang, J. Deng, X. Zhang, W. Liu, *ACS Nano* **2022**, *16*, 3119.

[8] M. J. Shen, K. Jiao, C. Y. Wang, H. Ehrlich, M. C. Wan, D. X. Hao, J. Li, Q. Q. Wan, L. Tonggu, J. F. Yan, *Adv. Sci.* **2022**, *9*, 2103693.

[9] M. J. Shen, C. Y. Wang, D. X. Hao, J. X. Hao, Y. F. Zhu, X. X. Han, L. Tonggu, J. H. Chen, K. Jiao, F. R. Tay, *Adv. Mater.* **2022**, *34*, 2107924.

[10] D. Van Der Spoel, E. Lindahl, B. Hess, G. Groenhof, A. E. Mark, H. J. Berendsen, *J. Comput. Chem.* **2005**, *26*, 1701.

[11] K. Vanommeslaeghe, E. Hatcher, C. Acharya, S. Kundu, S. Zhong, J. Shim, E. Darian, O. Guvench, P. Lopes, I. Vorobyov, *J. Comput. Chem.* **2010**, *31*, 671.

[12] A. D. MacKerell Jr, N. Banavali, N. Foloppe, *Biopolymers: original Research on biomolecules* **2000**, *56*, 257.

[13] P. Bjelkmar, P. Larsson, M. A. Cuendet, B. Hess, E. Lindahl, *J. Chem. Theory Comput.* **2010**, *6*, 459.

[14] T. Darden, D. York, L. Pedersen, *J. Chem. Phys.* **1993**, *98*, 10089.

[15] T.-J. Lin, H. Heinz, *J. Phys. Chem. C* **2016**, *120*, 4975.

[16] M. Parrinello, A. Rahman, *J. Appl. Phys.* **1981**, *52*, 7182.

[17] Y. Wang, J. Zhou, L. Yuan, F. Wu, L. Xie, X. Yan, H. Li, Y. Li, L. Shi, R. Hu, *Small* **2023**, *19*, 2206657.